A study of the $^{16}O(e,e'p)$ reaction at deep missing energies

N. Liyanage,[17] B. D. Anderson,[13] K. A. Aniol,[2] L. Auerbach,[29] F. T. Baker,[7] E. J. Beise,[16] J. Berthot,[1] W. Bertozzi,[17] P. -Y. Bertin,[1] L. Bimbot,[22] W. U. Boeglin,[5] E. J. Brash,[24] V. Breton,1 H. Breuer,[16] E. Burtin,[26] J. R. Calarco,[18] L. Cardman,[30] G. D. Cates,[23] C. Cavata,[26] C. C. Chang,[16] N. S. Chant,[16] J. -P. Chen,[30] E. Cisbani,[12] D. S. Dale,[14] A. Deur,[1] B. Diederich,[21] P. Djawotho,[33] B. Doyle,[14] J. -E. Ducret,[26] M. B. Epstein,[2] L. A. Ewell,[16] J. M. Finn,[33] K. G. Fissum,[17] H. Fonvieille,[1] B. Frois,[26] S. Frullani,[12] J. Gao,[17] F. Garibaldi,[12] A. Gasparian,[8,14] S. Gilad,[17] R. Gilman,[25] A. Glamazdin,[15] C. Glashausser,[25] J. Gomez,[30] V. Gorbenko,[15] T. Gorringe,[14] K. Griffieon,[33] F. W. Hersman,[18] R. Holmes,[28] M. Holtrop,[18] N. d'Hose,[26] C. Howell,[4] G. M. Huber,[24] C. E. Hyde-Wright,[21] M. Iodice,[12] C. W. de Jager,[30] S. Jaminion,[1] M. K. Jones,[33] K. Joo,[32] C. Jutier,[1,21] W. Kahl,[28] S. Kato,[34] J. J. Kelly,[16] S. Kerhoas,[26] M. Khandaker,[19] M. Khayat,[13] K. Kino,[31] W. Korsch,[14] L. Kramer,[5] K. S. Kumar,[23] G. Kumbartzki,[25] G. Laveissière,[1] R. De Leo,[10] A. Leone,[11] J. J. LeRose,[30] L. Levchuk,[15] M. Liang,[30] R. A. Lindgren,[32] G. J. Lolos,[24] R. W. Lourie,[27] R. Madey,[8,13,30] K. Maeda,[31] S. Malov,[25] D. M. Manley,[13] P. Markowitz,[5] D. J. Margaziotis[2] J. Marroncle,[26] J. Martino,[26] J. S. McCarthy,[32] K. McCormick,[21] J. McIntyre,[25] R. L. J. van der Meer,[24] Z. -E. Meziani,[29] R. Michaels,[30] J. Mougey,[3] S. Nanda,[30] D. Neyret,[26] E. A. J. M. Offermann,[30] Z. Papandreou,[24] C. F. Perdrisat,[33] R. Perrino,[11] G. G. Petratos,[13] S. Platchkov,[26] R. Pomatsalyuk,[15] D. L. Prout,[13] V. A. Punjabi,[19] T. Pussieux,[26] G. Quéméner,[33] R. D. Ransome,[25] O. Ravel,[1] Y. Roblin[1] R. Roché,[6] O. A. Rondon-Aramayo,[32] P. G. Roos,[16] D. Rowntree,[17] G. Rutledge,[33] P. M. Rutt,[25] A. Saha,[30] T. Saito,[31] A. J. Sarty,[6] A. Serdarevic-Offermann,[24] T. P. Smith,[18] A. Soldi,[20] P. Sorokin,[15] P. Souder,[28] R. Suleiman,[13] J. A. Templon,[7] T. Terasawa,[31] L. Todor,[21] H. Tsubota,[31] H. Ueno,[34] P. E. Ulmer,[21] G. Urciuoli,[12] P. Vernin,[26] S. van Verst,[17] B. Vlahovic,[20] H. Voskanyan,[35] J. W. Watson,[13] L. B. Weinstein,[21] K. Wijesooriya,[33] R. Wilson,[9] B. Wojtsekhowski,[30] D. G. Zainea,[24] V. Zeps,[14] J. Zhao,[17] Z. -L. Zhou,[17]

(The Jefferson Lab Hall A Collaboration)

[1] *Université Blaise Pascal/IN2P3, F-63177 Aubière, France*
[2] *California State University, Los Angeles, California, 90032*
[3] *Institut des Sciences Nucléaires, F-38026 Grenoble, France*
[4] *Duke University, Durham, North Carolina, 27706*
[5] *Florida International University, Miami, Florida, 33199*
[6] *Florida State University, Tallahassee, Florida, 32306*
[7] *University of Georgia, Athens, Georgia, 30602*
[8] *Hampton University, Hampton, Virginia 23668*
[9] *Harvard University, Cambridge, Massachusetts, 02138*
[10] *INFN, Sezione di Bari and University of Bari, I-70126 Bari, Italy*
[11] *INFN, Sezione di Lecce, I-73100 Lecce, Italy*
[12] *INFN, Sezione Sanitá and Istituto Superiore di Sanitá, Laboratorio di Fisica, I-00161 Rome, Italy*
[13] *Kent State University, Kent, Ohio, 44242*
[14] *University of Kentucky, Lexington, Kentucky, 40506*
[15] *Kharkov Institute of Physics and Technology, Kharkov 310108, Ukraine*
[16] *University of Maryland, College Park, Maryland, 20742*
[17] *Massachusetts Institute of Technology, Cambridge, Massachusetts, 02139*
[18] *University of New Hampshire, Durham, New Hampshire, 03824*
[19] *Norfolk State University, Norfolk, Virginia, 23504*
[20] *North Carolina Central University, Durham, North Carolina, 27707*
[21] *Old Dominion University, Norfolk, Virginia, 23559*
[22] *Institut de Physique Nucléaire, F-91406 Orsay, France*
[23] *Princeton University, Princeton, New Jersey, 08544*
[24] *University of Regina, Regina, Saskatchewan, Canada, S4S 0A2*
[25] *Rutgers, The State University of New Jersey, Piscataway, New Jersey, 08854*
[26] *CEA Saclay, F-91191 Gif-sur-Yvette, France*
[27] *State University of New York at Stony Brook, Stony Brook, New York, 11794*
[28] *Syracuse University, Syracuse, New York, 13244*
[29] *Temple University, Philadelphia, Pennsylvania, 19122*
[30] *Thomas Jefferson National Accelerator Facilty, Newport News, Virginia, 23606*
[31] *Tohoku University, Sendai 980, Japan*
[32] *University of Virginia, Charlottesville, Virginia, 22901*
[33] *College of William and Mary, Williamsburg, Virginia, 23187*
[34] *Yamagata University, Yamagata 990, Japan*

[35] *Yerevan Physics Institute, Yerevan 375036, Armenia*
(July 13, 1999)

The ^{16}O(e,e$'$p) reaction was studied in quasielastic kinematics at $q = 1000$ MeV and $\omega = 445$ MeV. R_L, R_T and R_{LT} response functions were extracted for $25 MeV < E_{miss} < 60$ MeV and $P_{miss} < 280$ MeV/c. For missing energies below 50 MeV and missing momenta below 150 MeV/c, the cross sections and the response functions are mostly accounted for by s-shell single particle knockout calculations. R_L becomes small for missing energies higher than 50 MeV suggesting the offset of the single particle interaction. R_T remains substantial in this region indicating non-single particle interactions. At $p_{miss} \approx 280$ MeV/c, R_L is consistent with zero and with theory. The cross section, R_T and R_{LT} are much bigger than DWIA single particle knockout calculations.

The (e,e$'$p) reaction in quasielastic kinematics ($\omega \approx Q^2/2m_p$ where Q and ω are the four-momentum and energy transfers) has long been a crucial tool in the study of nuclear structure. (e,e$'$p) cross section measurements have provided both a wealth of information on the wave functions of protons inside the nucleus and stringent tests of nuclear theories. Response function measurements have provided detailed information about the different reaction channels contributing to the cross section such as single- and multi-nucleon knockout, meson exchange currents, isobar excitations, and final state interactions.

In the first Born approximation the unpolarized (e,e$'$p) cross section can be expressed as [16]

$$\frac{d^6\sigma}{d\Omega_e d\Omega_p d\omega dE_{p'}} = \frac{p' E_{p'}}{(2\pi)^3}\sigma_{Mott}(V_L R_L + V_T R_T + V_{LT} R_{LT}\cos\phi + V_{TT} R_{TT}\cos 2\phi), \quad (1)$$

where V_L, V_T, V_{LT} and V_{TT} are kinematic factors dependent upon the electron vertex, ϕ is the angle between the electron scattering plane and the reaction plane, and σ_{Mott} is the Mott cross section.

In parallel kinematics, because the out-of-plane angle ϕ is not defined, only $R_{\rm L}$ and $R_{\rm T}$ survive in the expression for the cross section. Thus the Rosenbluth method may be used to separate R_L and R_T. In the case of perpendicular kinematics, all four terms are present in the expression for the cross section. By measuring the cross section on both sides of $\vec{q}$ ($\phi = 0°$ and $\phi = 180°$) keeping all other kinematic variables constant, $R_{\rm LT}$ can be extracted according to

$$R_{LT} = \frac{(2\pi)^3}{E'_p p'_p \sigma_{Mott}}\left[\frac{\sigma(0°) - \sigma(180°)}{2V_{LT}}\right] \quad (2)$$

The separation of $R_{\rm TT}$ requires an out-of-plane measurement. An in-plane Rosenbluth separation in the case of perpendicular kinematics allows for the separation of $R_L + \frac{V_{TT}}{V_L}R_{TT}$ and R_T.

Originally, the quasielastic cross section was attributed entirely to single particle knockout from the valence states of the nucleus. However, a series of ^{12}C(e,e$'$p) experiments performed at MIT-Bates [1], [2], [3], [4] which sampled various kinematic regions measured much larger cross sections at high missing energy ($E_{miss} = \omega - T_p$ where T_p is the final proton kinetic energy) than was expected for single particle knockout. Separated ^{12}C(e,e$'$p) data reported by Ulmer *et al* [1] show a dramatic increase in the transverse-to-longitudinal difference above the two-particle emission threshold. This enhancement suggests the presence of an additional, transverse, non-quasielastic reaction mechanism. The longitudinal response becomes consistent with zero above $E_{miss} = 50$ MeV, suggesting that single particle knockout is very small above this point. R_T/R_L enhancement above two-nucleon emission threshold has also been observed at NIKHEF-K for ^{6}Li [5] and ^{12}C [6]. More recently, a Jefferson lab hall C experiment has observed R_T/R_L enhancement above two-nucleon emission threshold for ^{12}C, ^{56}C and ^{197}Au [7]. These findings suggest that a significant part of the cross section at large missing energies arise due to two-body and multi-body processes.

There have been several theoretical attempts [8], [9], [10] to explain the continuum strength using many-body knockout models, but no model can explain all the data. It has also been suggested that short-range and tensor correlations could play a major role in populating the high E_{miss} continuum. Muther *et al.* [11] calculated the effects of these correlations in ^{16}O and have shown that they shift strength from conventional quasi-hole states to high-E_{miss}, high-P_{miss} channels.

In this experiment we measured the ^{16}O(e,e$'$p) reaction in the quasielastic region at $|\vec{q}| = 1000$ MeV and $\omega = 445$ MeV. We extracted the longitudinal (R_L), transverse (R_T) and longitudinal-transverse interference (R_{LT}) response functions from cross sections measured at several beam energies (E_0) and electron angles (θ_e) for $E_{miss} < 60$ MeV and $P_{miss} < 280$ MeV/c. This was the first Jefferson Lab Hall A experiment and the first response function separation on a complex nucleus at large (P_{miss}, E_{miss}). This paper reports the results for $E_{miss} > 25$ MeV.

We scattered the continuous incident electron beam from a waterfall target [12] and detected the scattered electrons in the High Resolution Electron Spectrometer (HRS$_e$) and the protons in the High Resolution Hadron Spectrometer (HRS$_h$). The details of the Hall A experimental setup are given in [13].

The waterfall target consisted of three flat flowing water 'foils', each approximately 130 mg/cm^2 thick along the beam and at 30° to the incident beam. Using three foils improved the target energy loss determination and allowed the use of vertex cuts to reject accidentals.

We measured the ^{16}O(e,e$'$p) cross-sections at three beam energies, 0.843, 1.643 and 2.442 GeV, keeping $|\vec{q}|$ and ω fixed, in order to vary the virtual photon polarization. At 2.442 GeV, we measured the cross section for six different proton-virtual photon angles, $\theta_{pq} = 0°, \pm 8°, \pm 16°$, and $\pm 20°$. At 0.843 GeV, we measured at $\theta_{pq} = 0°, +8°$, and $+16°$. $\theta_{pq} = 0°$ and $\pm 8°$ measurements at 1.643 GeV provided redundancy for checking systematic uncertainties. These measurements allowed us to separate R_L and R_T at $\theta_{pq} = 0°$ and $R_L + \frac{V_{TT}}{V_L}R_{TT}, R_T$ and R_{LT} at $\theta_{pq} = 8°$ and 16°.

The accuracy of a response function separation depends on matching the values of $|\vec{q}|$ and ω between different kinematic settings. In order to match $\vec{q}$, we measured H(e,e$'$p) (also present in the waterfall target) with a pinhole collimator on HRS$_e$. The momentum of the detected protons is equal to $\vec{q}$. We determined the location of the H(e,e$'$p) momentum peak to $\frac{\delta p}{p} = 2 \times 10^{-4}$ allowing us to match $|\vec{q}|$ to 2×10^{-4} between different kinematic settings. Throughout the experiment H(e,e′) data, measured simultaneously with the ^{16}O(e,e′p) data, provided a continuous monitor of luminosity and beam energy. The radiation corrections to the measured cross sections were performed using the code RADCOR [14], [15], [13] which unfolds the radiative tails in the E_{miss} P_{miss} space.

For the "parallel" kinematic setting of this experiment ($\theta_{pq} = 0°$) the H(e,e′p) peak and the associated radiative tail were present in the coincidence phase-space for ^{16}O. To remove H(e,e′p) events we cut out all events with $P_{miss} < 45$ MeV/c. This cut significantly reduced the ^{16}O(e,e′p) statistics for this setting removing a large fraction of the events with $\vec{P}_{miss} \parallel \vec{q}$. However, since the remaining events have $\vec{P}_{miss}$ symmetrically distributed around $\vec{q}$ with $\theta_{pq} < 1.5°$, this data sample is approximately parallel, in that the interference response functions, which depend on ϕ (the azimuthal angle around $\vec{q}$), average out to zero. Still, due to this problem we call this setting "quasi-parallel" kinematics. The perpendicular kinematic settings had no contamination due to H.

To check how much of the observed continuum strength can be explained by $1s_{1/2}$ knockout, we compared our results to $1s_{1/2}$ single particle knockout calculations by Van Orden [17], [18], Kelly [16] and Ryckebusch [19], [20], [21]. The Ryckebusch calculations (Impulse Approximation (IA) calculations and calculations that include two-body current contributions related to MEC and IC) have been performed in a self-consistent Hartree-Fock (HF) frame work. Kelly's calculations are non-relativistic DWIA (Distorted Wave Impulse Approximation) while Van Orden's calculations are relativistic DWIA. For all calculations, we distributed the calculated $1s_{1/2}$ response functions in E_{miss} using a prescription given by Jeukenne and Mahaux [22], [8], where the $1s_{1/2}$ profile is modeled using a Lorentzian shape with an energy-dependent width $\Gamma(E)$.

Fig. 1 shows the cross sections measured over the whole range of missing momenta covered by this experiment. The cross sections are compared to $1s_{1/2}$ single particle knockout calculations by Van Orden [17], [18] folded in with the energy dependent Lorentzian parameterization by Mahaux. At $\langle P_{miss} \rangle = 50$ MeV, the Lorentzian shape exactly describes the measured cross section. We determined the normalization factor used with all Van Orden calculations presented here by fitting to this data. For the $1s_{1/2}$-shell the normalization factor thus determined was 0.88. Note that this is significantly higher than the previously reported normalization factors for the $1s_{1/2}$-shell [23].

As P_{miss} increases, the single particle knockout calculation accounts for only a fraction of the measured strength. Furthermore, for the two settings with P_{miss} above the Fermi momentum of oxygen ($\approx$ 220 MeV/c), the measured cross section profiles do not exhibit any resemblance to the expected $1s_{1/2}$ Lorentzian shape. This clearly indicates that the cross section measured at high P_{miss} and high E_{miss} is mostly of non-single particle origin.

Figs. 2 - 4 present the separated response functions from this experiment for $|\theta_{pq}| = 0, 8°$ and $16°$ corresponding to missing momenta of approximately 60, 145 and 280 MeV/c. Fig. 2 presents the separated response functions for the "quasi-parallel" kinematic setting. The wide peak centered around $E_{miss} = 40$ MeV in both R_L and R_T corresponds primarily to single particle knockout from the $1s_{1/2}$ state. The difference between the transverse and longitudinal spectral functions $(S_T - S_L)$[1], which is expected to be zero for a free nucleon, is nonzero for $E_{miss} > 40$ MeV. This is in qualitative agreement with the high E_{miss} behavior of R_L and R_T observed at MIT-Bates by Ulmer *et al.* [1] and also at Jefferson lab Hall C [7]. However, the uncertainties on $S_T - S_L$ are too large to draw any conclusions about the onset of the difference.

Fig. 3 presents the separated response functions for the $|\theta_{pq}| = 8°$ perpendicular kinematic setting, ($p_{miss} \approx 145$ MeV/c). At this setting R_T is approximately constant for the entire range of missing energy measured ($25 < E_{miss} < 60$ MeV) whereas $R_L + V_{TT}R_{TT}/V_L$ is consistent with zero for $E_{miss} > 50$ MeV. Since $\frac{V_{TT}}{V_L}R_{TT}$ is estimated to be about 7% of R_L [17], [18], this behavior can be attributed mainly to R_L. The Mahaux parameterization does not reproduce the missing energy shape of R_L or R_T. For $E_{miss} < 35$ MeV, all calculated response functions underestimate data. For $E_{miss} > 50$ MeV, $R_L + \frac{V_{TT}}{V_L}R_{TT}$ is consistent with both zero and the calculations. R_T, on the other hand, appears to retain strength above 50 MeV. This is in agreement with the parallel kinematics results of the present experiment and also with the results from Bates and Hall C. R_{LT} is about twice as large as all three calculations over the whole range of E_{miss}. At this $|\theta_{pq}|$ setting R_{LT} was calculated separately from the data acquired at the beam energy values of 1.643 GeV and 2.442 GeV. At each E_{miss} bin the R_{LT} values calculated for the two beam energies agree well within statistical error. This indicates that the systematic errors for the experiment are smaller than the statistical errors.

Fig. 4 presents the separated response functions for the $|\theta_{pq}| = 16°$, $p_{miss} \approx 280$ MeV/c setting. At this setting, R_T and R_{LT} appear to slowly decrease over $25 < E_{miss} < 60$ MeV. $R_L + V_{TT}R_{TT}/V_L$ is close to zero as expected by all three calculations. However, R_T and R_{LT} are much larger than the DWIA calculation and ap-

[1] $S_L = \frac{\sigma_M V_L R_L}{\sigma_L^{ep}}$, $S_T = \frac{\sigma_M V_T R_T}{\sigma_T^{ep}}$, where σ_L^{ep} and σ_T^{ep} are the longitudinal and transverse parts of the off-shell ep cross section obtained using deForest's CC1 prescription.

proximately as large as the HF-RPA calculation. Neither R_T nor R_{LT} show a peak at $E_{miss} \approx 40$ MeV corresponding to single particle knockout from the s-shell. Note that the high strength predicted by the HF calculation at this value of P_{miss} does not arise from the two-body current contributions included in the HF calculation. It has been shown that the (e,e′pn) and (e,e′pp) contributions calculated by Ryckebusch *et al.* account for only a small fraction of the excess continuum strength observed in this experiment and in previous experiments [8], [13].

In summary, at low missing momenta ($p_{miss} < 75$ MeV/c) and low missing energies $E_{miss} < 50$ MeV) the DWIA $1s_{1/2}$ single particle knockout calculations account for most of the observed continuum strength. However, as one moves to high missing momenta or high missing energies, the observed cross sections become higher than the DWIA single particle knockout predictions. Most of this excess strength appears to reside in transverse (R_T) and longitudinal-transverse interference (R_{LT}) channels while the longitudinal component (R_L) is consistent with the calculations. While the cross section and the response functions measured at $p_{miss} < 75$ MeV/c agree well with the expected $1s_{1/2}$ Lorentzian shape, the cross sections measured at missing momenta higher than the Fermi momentum do not exhibit any resemblance to this Lorentzian shape. These observations suggest that the cross section measured at high P_{miss} and high E_{miss} is mostly of non-single particle origin.

---

[1] P.E. Ulmer *et al.,* Phys. Rev. Lett. **59,** 2259 (1987).
[2] R. Lourie *et al.,* Phys. Rev. Lett. **56,** 2364 (1986).
[3] L. Weinstein *et al.,* Phys. Rev. Lett. **64,** 1646 (1990).
[4] J.H. Morrison, Phys. Rev. C **59,** 221 (1999).
[5] J.B.J.M. Lanen *et al.,* Phys. Rev. Lett. **64,** 2250 (1990).
[6] G. van der Steenhoven *et al.,* Nucl. Phys. **A480,** 547 (1988).
[7] D. Dutta, Ph.D. thesis, Northwestern University (1999).
[8] J. Ryckebusch *et al.,* Nucl. Phys. **A624,** 581 (1997).
[9] A. Gil *et al.,* Nucl. Phys. **A627,** 599 (1997).
[10] T. Takaki, Phys. Rev. C **39,** 359 (1989).
[11] H. Muther and W.H. Dickhoff *et al.,* Phys. Rev. C **49,** R17 (1994).
[12] F. Garibaldi *et al.,* Nucl. Instrum. Methods **A314,** 1 (1992).
[13] N. Liyanage, Ph.D. thesis, MIT (1999).
[14] E. Quint, Ph.D. thesis, University of Amsterdam (1988).
[15] R. Florizone, Ph.D. thesis, MIT (1999).
[16] J.J. Kelly, Adv. Nucl. Phys., **23** ed. by J.W. Negele and E. Vogt 75 (1996).
[17] A. Picklesimer, J. W. Van Orden, and S. J. Wallace, Phys. Rev. C **32**, 1312 (1985).
[18] A. Picklesimer and J. W. Van Orden, Phys. Rev. C **40**, 290 (1989).
[19] J. Ryckebusch *et al.,* Nucl. Phys. **A476,** 237 (1988).
[20] J. Ryckebusch *et al.,* Nucl. Phys. **A503,** 694 (1989).
[21] V. Van der Sluys, K. Heyde, J. Ryckebusch, M. Waroquier, Phys.Rev. C **55** (1997) 1982
[22] J.P. Jeukenne and C. Mahaux, Nucl. Phys. **A394,** 445 (1983).
[23] W. Bertozzi, Nucl. Phys. **A527,** 347 (1991).

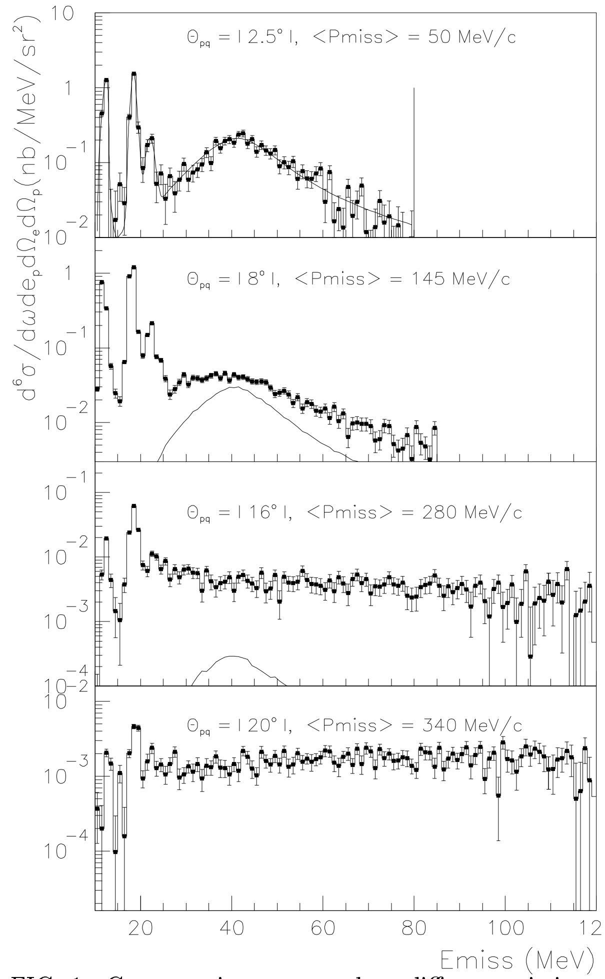

FIG. 1. Cross section measured at different missing momenta as a function of missing energy. The solid lines show the $1s_{1/2}$ single particle strength calculated by Van Orden folded with the energy dependent Lorentzian parameterization by Mahaux. The s-shell spectroscopic factor used with the calculation was determined by fitting to the $\theta_{pq} = 2.5°$ data (top plot)

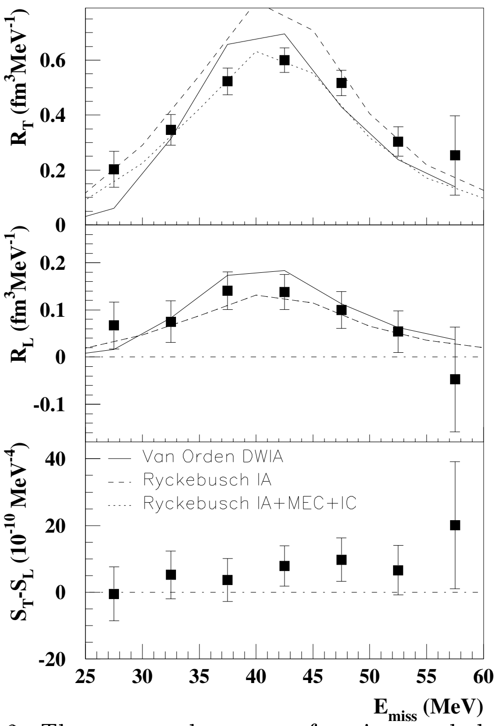

FIG. 2. The separated response functions and the difference of the longitudinal and transverse spectral functions for quasi-parallel kinematics for 45 MeV/c $< p_{miss} <$ 75 MeV/c. Note that the calculations have been binned in the same manner as the data

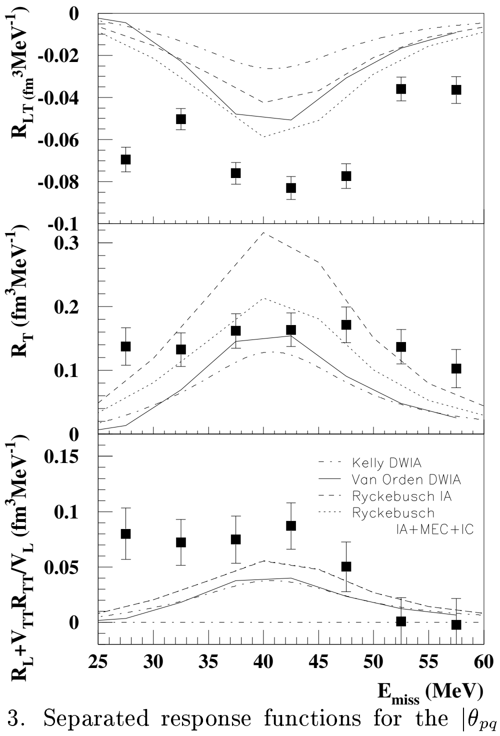

FIG. 3. Separated response functions for the $|\theta_{pq}| = 8°$ setting ($P_{miss}^{average} \approx 145$ MeV/c). Plots show (from top to bottom) R_{LT}, R_T, and $R_L + \frac{V_{TT}}{V_L} R_{TT}$.

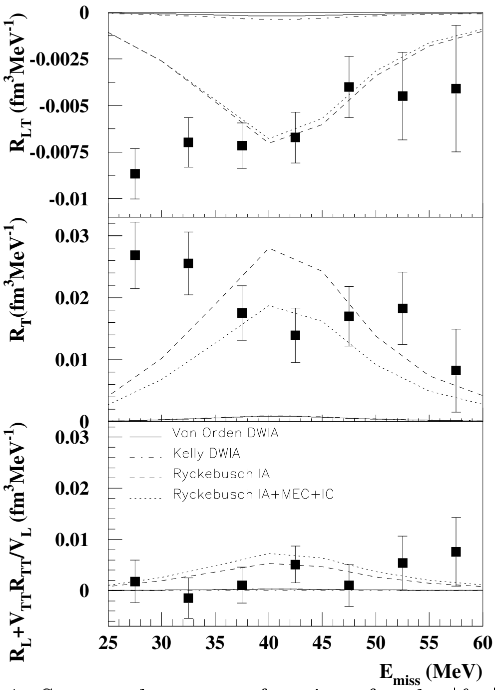

FIG. 4. Separated response functions for the $|\theta_{pq}| = 16°$ setting ($P_{miss}^{average} \approx 280.0$ MeV/c). Plots show (from top to bottom) R_{LT}, R_T, and $R_L + \frac{V_{TT}}{V_L} R_{TT}$.